Solubility of Potassium Hydroxide and Potassium Phosphate in Supercritical Water

William T. Wofford,*,† Philip C. Dell'Orco,‡ and Earnest F. Gloyna†

Environmental and Water Resources Engineering, Department of Civil Engineering, The University of Texas at Austin, Austin, Texas 78712, and Chemical and Laser Sciences Division, Los Alamos National Laboratory, Los Alamos, New Mexico 87545

The solubilities of potassium hydroxide and dibasic potassium phosphate in supercritical water solutions have been measured at temperatures from 400 to 525 °C and pressures from 22.1 to 32.0 MPa. The solubility of potassium hydroxide varied from 61 mg/kg at 525 °C and 22.1 MPa to 594 mg/kg at 450 °C and 30.4 MPa. The solubility of dibasic potassium phosphate varied from 2 mg/kg at 450 °C and 26.8 MPa to 416 mg/kg at 400 °C and 27.1 MPa. The solubility was found to vary directly with pressure and inversely with temperature. Results were fit to a semiempirical solvation model to yield predictive equations for solubility as a function of water density.

Introduction

These studies were motivated by applications for electrolyte solubility data in the supercritical water oxidation process. Supercritical water oxidation (SCWO) is an emerging technology for the thermal destruction of organic compounds in wastewaters and sludges. SCWO utilizes the unique properties of water above its critical point (374.2 °C, 22.1 MPa) to rapidly oxidize organic compounds into simple innocuous byproducts such as carbon dioxide and water.

A characteristic of supercritical water which is advantageous for achieving complete and rapid oxidation of organic compounds is the high solubility exhibited by nonpolar organics and gases (Connolly, 1966). Nonpolar compounds which are normally insoluble in water at room temperature are nearly completely miscible at typical SCWO operating conditions (400–525 °C, 25–35 MPa) due to the greatly reduced density, dielectric constant, and ionization constant of supercritical water. The nonpolar-solvent character of supercritical water permits SCWO reactants to occupy a single phase and reactions to proceed independent of mass transfer limitations.

The properties of supercritical water which make it an excellent solvent for nonpolar organic compounds make it a poor solvent for polar inorganic compounds (Martynova, 1976). Solubility is reduced to such an extent that many electrolytes can be effectively removed from wastewaters during SCWO treatment through precipitation and solids separation (Dell'Orco, 1993). However, the formation of a separate solid or liquid phase may affect destruction efficiencies and cause plugging or fouling of the process equipment. Thus, effective implementation of SCWO technology requires detailed knowledge of the solubility properties of the wastes to be treated.

In this paper, data are presented for the solubility of potassium hydroxide (KOH) and dibasic potassium phosphate (K_2HPO_4) in supercritical water at conditions common to the SCWO process.

Experimental Approach

The goal in solubility studies is to achieve an equilibrium separation between the solvent media and the concentrated solute phase. A common method for determining solubility in supercritical water (SCW) involves passing SCW through a salt bed and allowing the salt to saturate the SCW to its equilibrium concentration (Martynova, 1976; Marshall, 1968; Galobardes, 1981). The effluent from the salt bed is cooled, depressurized, and then analyzed for the electrolyte. The salt bed works well for high-melting compounds (>600 °C), such as sodium chloride and sodium sulfate. However, the alkali hydroxides and alkali phosphates do not lend themselves to this method due to their low melting points. At supercritical temperatures, potassium hydroxide (mp, 360.4 °C) and potassium phosphate (mp, <300 °C) exist as a liquid-melt. A large mass of molten salt has a tendency to be transported with the supercritical vapor phase, contaminating the effluent samples. An impermeable salt solution may also cause short circuiting of the SCW or plugging of the solubility apparatus.

As a result of these problems, Dell'Orco (1994) developed a new method to determine the solubility of alkali nitrates. This method takes advantage of the fact that nucleation and precipitation reactions can occur rapidly in SCW. Electrolyte solutions are heated above their saturation temperature in a low flow velocity (~1 cm/s) and long residence time (50–120 s) apparatus. Excess electrolyte is precipitated as a separate phase, leaving the effluent SCW phase at its solubility limit. The precipitated electrolyte settles to the bottom of the separation vessel. An outlet filter is used to trap any solids which are not retained within the vessel. In this approach, the problems of carryover and plugging are minimized by maintaining a small volume of molten salt within the apparatus.

The phase behavior of salt–water systems at high temperature depends upon both the nature of the salt and its initial concentration. Salts are often classified as type I or type II based on how their liquid phase solubility changes with increasing temperature in a binary salt–water system saturated with the salt (Valyashko, 1976). Type I salts are characterized by a continuously increasing solubility along the liquid-solid equilibrium curve of the system's phase diagram. Potassium phosphate is a type I salt (Valyashko, 1976; Marshall, 1982). On the basis of potassium hydroxide's low melting point and high solubility in water, it is reasonable to assume that it will also exhibit type I solubility behavior. Saturated solutions of type I salts follow a "nonaqueous" solvation mechanism in which

* The University of Texas at Austin.
‡ Los Alamos National Laboratory.

0021-9568/95/1740-0968$09.00/0

the interactions between salt molecules play an important role and in which liquid phase solubility increases with increasing temperature. Exceptions to this behavior occur in dilute solutions (below the solution's critical composition) where interactions between salt molecules are insignificant and the mechanism of solvation is determined by water–water and water–salt interactions. In this situation, the solubility of the salt will decrease with increasing temperature as water changes from a polar to a nonpolar solvent.

For this study, and for most SCWO applications, feed solutions contain low concentrations of salts and are far removed from saturation conditions at room temperature. Thus, these dilute salt–water systems do not follow the liquid–solid equilibrium curve as they are heated but rather remain as single-phase fluids up to the point where the saturation temperature is finally exceeded. After phase separation occurs, the system follows either the vapor–liquid or vapor–solid equilibrium curves of the phase diagram. Within the temperature and pressure range covered by this study, the equilibrium concentration of electrolyte in the dilute vapor (or supercritical fluid) phase decreases with increasing temperature.

The critical temperature of a salt–water mixture is also strongly dependent upon composition. Critical point data for the system K_2HPO_4–H_2O indicate that the dilute (<1 mass %) solutions of K_2HPO_4 used here are supercritical at experimental conditions (Marshall et al., 1981; Marshall, 1982). These studies reported a vapor–liquid critical curve starting at 374 °C for pure water and ending at approximately 377 °C and 3 mass % K_2HPO_4. Critical point data was not available for the system KOH–H_2O. However, the data for the system K_2HPO_4–H_2O suggest that the critical point of a dilute solution of KOH is close to that of pure water and, in any case, well below the lowest experimental temperature of 423 °C.

Experimental Procedure

The solubility studies were conducted using a laboratory-scale, continuous-flow apparatus based on the work of Dell'Orco (1994). Primary features of the apparatus included a preheat section; a positive temperature-gradient, packed-bed column in which precipitation occurred; and a filter following the column. A schematic diagram of the apparatus is shown in Figure 1. All components and tubing were constructed of Type 316 stainless steel. The precipitation chamber was constructed of Autoclave Engineers medium-pressure tubing (30.5 cm long, 2.54 cm o.d., and 1.43 cm i.d.) and filled with packing material consisting of either ceramic beads or nickel wire. A Nupro relief valve (Series R3A), located after the chill water cooler, served as a back-pressure regulator. The system pressure was measured prior to letdown with an accuracy of ±0.02 MPa by an Ashcroft transducer (Model K1). The fluid temperatures at the inlet and outlet of the column/filter assembly (T5 and T10 in Figure 1) were measured with Omega K-type thermocouples with accuracies of ±0.5 °C. A PID temperature controller (Omega Model 4401), connected to thermocouple T10, regulated electrical power to the radiant heater so as to maintain a constant temperature at the outlet. The remaining thermocouples measured wall temperatures and were used to monitor the temperature gradients within the preheater and precipitation chamber.

Electrolyte solutions were fed to the apparatus using a HPLC pump (LDC Analytical) operating at a constant flow rate of 3 mL/min. For the present studies, the concentration of electrolyte in the feed solution varied between 0.1 and 0.2 mass %. The lower limit on the feed concentration was based on previous experience with this method

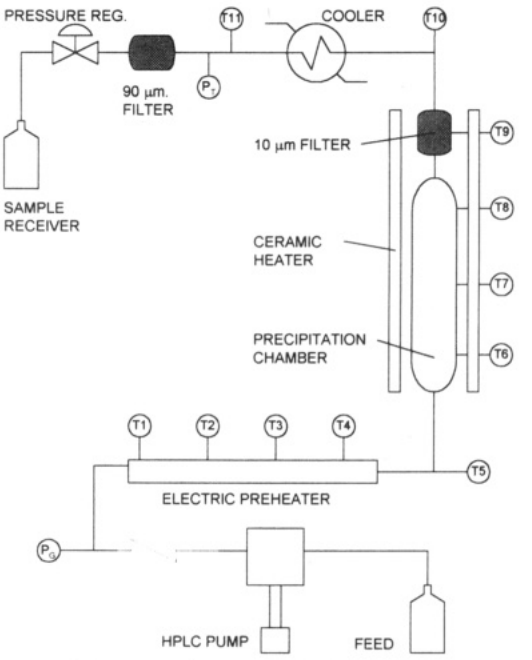

Figure 1. Schematic diagram of solubility apparatus: T#, thermocouple; P_T, pressure transducer; P_G, pressure gauge.

(Dell'Orco, 1994). It was observed that a feed concentration which was at least three times greater than the expected solubility in SCW was necessary in order to ensure that sufficient electrolyte was present to establish equilibrium between the electrolyte in the supercritical fluid (SCF) phase and that in the precipitated phase. The upper limit on the feed concentration was based on two considerations. First, a concentration as low as practical was desired to avoid plugging and/or channeling within the precipitation chamber. Second, the presence of a high concentration of electrolyte in either the SCF phase or precipitated phase could affect the desired equilibrium. For example, high concentrations (>0.1 M) of NaOH have been observed to enhance the solubility of phosphates in hydrothermal systems (Valyashko, 1976). The feed solution was preheated to approximately 350 °C prior to entering the precipitation column. A subcritical temperature was chosen for the preheater outlet to ensure that the majority of electrolyte remained soluble prior to entering the precipitation chamber, thereby reducing the possibility of plugging the tubing which connected the preheater and precipitation chamber. The solution then moved upward through the packed bed while being heated to the desired supercritical temperature. The purpose of the packing material was to provide a large, nonreactive surface area for nucleation and precipitation. Electrolyte in excess of the solubility limit for the temperature at a given height within the column was precipitated as a separate liquid phase. Separation of this dense salt phase from the SCF phase was accomplished using a combination of gravity settling and surface tension between the packing material and electrolyte. In dilute aqueous solutions, potassium hydroxide and potassium phosphate exhibited negative temperature coefficients of solubility (i.e., solubility decreased with increasing temperature) so that in these experiments the minimum solubility occurred at the top of the column/filter assembly.

The saturated effluent from the column/filter assembly was cooled, depressurized, and sampled for analysis. Cation concentrations were measured with a Perkin-Elmer Plasma 40 inductively coupled plasma spectrometer (ICP). The typical detection limit for potassium on the ICP

instrument was 0.1 mg/kg. Anion concentrations were measured using a Dionex System 14 ion chromatograph operated with an IonPac AS3 column and carbonate eluent. Phosphate concentrations down to 1.0 mg/kg could be accurately detected with this instrument. The concentrations of hydronium and hydroxide ions were determined from the pH of samples as measured using an Orion Research pH electrode (Model 98-06).

Between eight and twelve samples were collected and analyzed for each set of experimental conditions over a period of 90−120 min. The solubility of KOH was determined from the average potassium concentration measured at steady state. Similarly, the solubility of K_2HPO_4 was determined from the average steady-state concentration of phosphate. The choice of phosphate rather than potassium for this determination is discussed later. The experimental temperature and pressure were also determined from the average of steady-state values recorded during sample collection at 5 min intervals. In each case, the standard deviation of the measurements was used to approximate the error. The standard deviations for potassium and phosphate measurements are given in the results section. Standard deviation of the steady state temperature was ±0.5 °C. Pressure was controlled manually with the backpressure regulator within ±0.4% of the mean. Water density at the average temperature and pressure was taken from steam tables (Haar and Gallagher, 1984). The maximum uncertainty in the calculated water density, resulting from the cumulative effect of temperature and pressure variation, was approximately ±0.001 g·cm^{-3} (0.06 mol·L^{-1}).

Material corrosion was monitored by analyzing effluent and rinse water samples by ICP for iron, nickel, chromium, and molybdenum, the major elemental components of stainless steel. Representative effluent samples were also analyzed by ICP for aluminum to evaluate the condition of the α-alumina ceramic beads used as a packing material in the KOH studies.

The effect of flow rate on solubility measurements was investigated during four experiments conducted at 450 °C and 27.6 MPa. An additional experiment was conducted in a 1 L batch reactor (Autoclave Engineers) to obtain a solubility value at the limiting condition of zero flow. The tests showed no significant change in solubility at flow rates up to 5 mL/min. In some experiments, breakthrough of the precipitated electrolyte phase was observed at flow rates > 5 mL/min.

Materials

The potassium hydroxide and dibasic potassium phosphate were reagent grade chemicals manufactured by J. T. Baker, Inc. The potassium hydroxide had a stated purity of 99+ mass % and the potassium phosphate had a stated purity of 98.9 mass %. Potassium internal standards were prepared from reagent grade potassium chloride manufactured by J. T. Baker, Inc., with a stated purity of 99.3 mass %. These chemicals were used without further purification. Phosphate internal standards were prepared from a 1000 mg/mL ± 5 μg/mL stock solution manufactured by High-Purity Standards. The water was laboratory distilled and deionized.

Two types of packing materials were used for these studies. For the potassium hydroxide studies, the packing material consisted of 0.56 cm diameter α-alumina ceramic beads (Coors Ceramics). The caustic conditions of the potassium hydroxide studies caused some dissolution of the ceramic beads which resulted in a buildup of alumina particles at the bottom of the precipitation chamber. For the potassium phosphate studies, the ceramic beads were replaced with $^1/_{16}$ in. diameter nickel wire (99+ % Ni), cut into $^1/_4$ in. lengths. The nickel wire withstood the caustic conditions while still providing a large surface area for precipitation.

Table 1. Comparison of Sodium Chloride Solubilities from This Work with Those from the Model Prediction of Pitzer and Pabalan (1986)

		s/(mg·kg^{-1})	
t/°C	P/MPa	this work	model prediction
450	24.8	233	279
470	25.0	195	215

Table 2. Solubility of Potassium Hydroxide in Supercritical Water

t/°C	P/MPa	ϱ/(g·cm^{-3}) (mol·L^{-1})	K/(mg·kg^{-1}) (±SD[a])	$10^3 s$/(mol·kg^{-1}) (±SD[a])
423	22.2	0.104 (5.78)	78.7 ± 2.1	2.01 ± 0.05
425	26.2	0.139 (7.72)	210 ± 11	5.37 ± 0.28
425	22.1	0.102 (5.67)	113 ± 20	2.89 ± 0.51
450	27.6	0.128 (7.11)	226 ± 11	5.78 ± 0.28
450	27.7	0.129 (7.17)	231 ± 17	5.91 ± 0.43
450	27.8	0.129 (7.17)	231 ± 3	5.91 ± 0.08
450	30.4	0.152 (8.44)	414 ± 6	10.6 ± 0.15
450	28.4	0.135 (7.50)	206 ± 12	5.27 ± 0.31
472	22.4	0.085 (4.72)	54.5 ± 2.7	1.39 ± 0.07
475	25.3	0.099 (5.50)	107 ± 5	2.74 ± 0.13
475	22.3	0.084 (4.67)	53.6 ± 3.1	1.37 ± 0.08
475	29.1	0.123 (6.83)	175 ± 7	4.48 ± 0.18
500	24.9	0.090 (5.00)	73.9 ± 4.3	1.89 ± 0.11
500	26.6	0.098 (5.44)	80.9 ± 3.2	2.07 ± 0.08
500	29.1	0.111 (6.17)	142 ± 3	3.63 ± 0.08
525	22.1	0.072 (4.00)	42.5 ± 2.4	1.09 ± 0.06

[a] SD = standard deviation.

Table 3. Solubility of Potassium Phosphate (K_2HPO_4) in Supercritical Water

t/°C	P/MPa	ϱ/(g·cm^{-3}) (mol·L^{-1})	K/(mg·kg^{-1}) (±SD[a])	PO_4/(mg·kg^{-1}) (±SD[a])	$10^4 s$[b]/(mol·kg^{-1}) (±SD[a])
400	24.9	0.165 (9.17)	41.3 ± 4.6	32 ± 6	3.4 ± 0.6
400	27.0	0.219 (12.2)	222 ± 17	222 ± 20	23.4 ± 2.1
400	27.1	0.224 (12.4)	202 ± 14	227 ± 14	23.9 ± 1.5
425	27.6	0.156 (8.67)	18.3 ± 0.5	11 ± 1	1.2 ± 0.1
425	29.1	0.175 (9.72)	42.7 ± 1.7	17 ± 1	1.8 ± 0.1
425	30.3	0.192 (10.6)	49.3 ± 6.2	38 ± 5	4.0 ± 0.5
425	30.9	0.204 (11.3)	59.6 ± 4.2	54 ± 3	5.7 ± 0.3
450	26.8	0.122 (6.78)	6.4 ± 0.6	1.0 ± 0.3	0.10 ± 0.03
450	28.0	0.131 (7.28)	4.9 ± 0.3	1.7 ± 0.3	0.18 ± 0.03
450	29.5	0.144 (8.00)	13.2 ● 1.2	3.8 ± 2.0	0.40 ± 0.2
450	30.4	0.152 (8.44)	10.9 ± 1.1	4.2 ± 0.2	0.44 ± 0.02

[a] SD = standard deviation. [b] Solubility is based on measured PO_4 concentration.

Results and Discussion

The reliability of the experimental procedure was first tested by measuring the solubility of sodium chloride (NaCl) at two points in the supercritical region and comparing with values reported in the literature. Table 1 shows the results of these experiments. The measured solubilities are in good agreement with the literature values (Pitzer and Pabalan, 1986). It should be noted that the solubility values for NaCl were based on chloride ion measurements. The accuracy of using chloride concentration to calculate NaCl solubility is affected by the degree of hydrolysis which occurs. The work of Armellini and Tester (1993) suggested that NaCl hydrolysis was negligible for temperatures between 400 and 500 °C and pressures from 15.0 to 30 MPa.

Tables 2 and 3 show the measured concentrations of potassium and phosphate and the corresponding molar

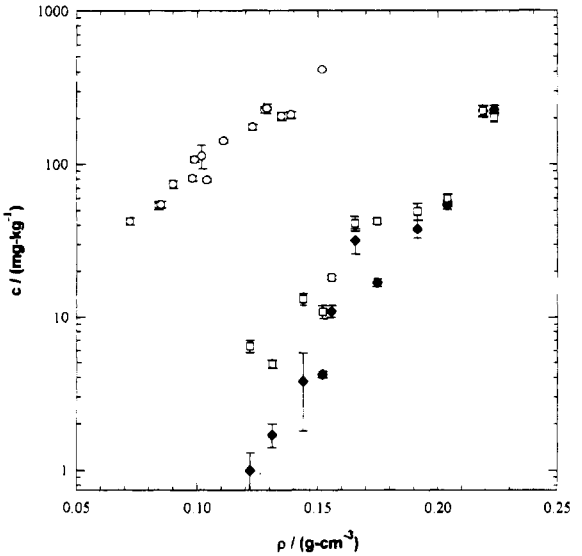

Figure 2. Concentrations of potassium and phosphate measured in the KOH study (○) and the K_2HPO_4 study (□, ◆) as a function of water density.

solubilities for KOH and K_2HPO_4. The experimental data and associated error bars are shown graphically as a function of water density in Figure 2. Error bars are based on the standard deviation of samples taken at steady state. Solubility values from replicate experiments made at 450 °C and 27.7 ± 0.1 MPa for the KOH study and at 400 °C and 27.1 MPa for the K_2HPO_4 study were within ±1.5% of their respective means, indicating good experimental reproducibility.

The solubility of KOH varied from 1.09×10^{-3} mol·kg^{-1} at 525 °C and 22.1 MPa to 10.6×10^{-3} mol·kg^{-1} at 450 °C and 30.4 MPa. These results are consistent with the limited solubility data available for other alkali hydroxides and alkali salts. In general, solubility is expected to decrease with increasing cation size: Li → Na → K → Ca (Dell'Orco, 1994). For example, the solubility of calcium hydroxide at 450 °C and 30 MPa is approximately 3.5×10^{-7} mol·kg^{-1} (Martynova, 1976), nearly 5 orders of magnitude below that of potassium hydroxide. Direct comparison between KOH and sodium hydroxide (NaOH) is not possible because the solubility of NaOH in SCW has not been studied for solution concentrations below 2 mass %. However, data are available for NaCl at these conditions. Furthermore, vapor pressure measurements of NaOH and NaCl solutions made at concentrations between 2 and 50 mass % and temperatures between 350 and 500 °C suggest that the solubility and NaOH and NaCl converge at concentrations below 2 mass % (Urusova, 1974). In this case, the solubilities of KOH can be compared directly with the literature values for NaCl. The solubilities of NaCl are, as predicted from cation size considerations, higher than those reported here for KOH. Typical values for NaCl range from 1.2×10^{-3} mol·kg^{-1} (525 °C, 22 MPa) to 17.3×10^{-3} mol·kg^{-1} (450 °C, 30 MPa) (Armellini and Tester, 1993; Pitzer and Pabalan, 1986).

The solubility of K_2HPO_4 varied from 1.0×10^{-5} mol·kg^{-1} at 450 °C and 26.8 MPa to 2.39×10^{-3} mol·kg^{-1} at 400 °C and 27.1 MPa. The molar ratio of potassium to phosphate (K/PO_4) in the effluent varied inversely with density, increasing from a value of 2.2 at a density of 12 mol·L^{-1} (0.22 g·cm^{-3}) to a value of 11 at a density of 6.8 mol·L^{-1} (0.12 g·cm^{-3}). In the absence of any side reactions, the K/PO_4 ratio would equal two, corresponding to the molar ratio present in K_2HPO_4. The observed deviations from this ideal value can be explained by the hydrolysis of potassium phosphate to form potassium hydroxide:

$$K_3PO_4 + H_2O \rightleftharpoons KOH + K_2HPO_4 \quad (1)$$

$$K_2HPO_4 + H_2O \rightleftharpoons KOH + KH_2PO_4 \quad (2)$$

$$KH_2PO_4 + H_2O \rightleftharpoons KOH + H_3PO_4 \quad (3)$$

Hydrolysis reactions 1–3 are written for the supercritical fluid phase, omitting the hydration water associated with each electrolyte species. It is evident from Figure 2 that potassium hydroxide has a higher solubility than potassium phosphate. Thus, hydrolysis reactions 1 and 2 served to transfer the potassium ion from relatively insoluble potassium phosphate species to a more soluble form, potassium hydroxide. Reaction 3 did not have an affect on the K/PO_4 ratio due to the high solubility of phosphoric acid relative to the other species. The overall effect of hydrolysis was to increase the ratio of potassium to phosphate in the effluent above the expected value of two. Hydrolysis was most significant at lower water densities where the solubility of potassium phosphate was low and the relative amount of potassium hydroxide was high. The presence of potassium hydroxide in the effluent required that the solubility of potassium phosphate be determined from the concentration of phosphate rather than potassium.

Additional evidence for the hydrolysis of phosphate salts was provided by Marshall and Begun (1989) based on Raman spectra of aqueous sodium phosphate solutions at temperatures up to 450 °C. The Raman spectra confirmed that at supercritical conditions a dilute salt phase existed in equilibrium with a concentrated liquid–melt phase containing most of the phosphate salt. They reported that Na_3PO_4 was entirely hydrolyzed at 200 °C. Both Na_2HPO_4 and NaH_2PO_4 were stable toward hydrolysis for 20 h at 320 °C. However, hydrolysis of these compounds may occur at supercritical temperatures. The Raman spectra suggest that the hydrolysis of K_3PO_4, and to some extent K_2HPO_4, occurred at the conditions of the present studies. In addition, Marshal and Begun found some spectral evidence for the polymerization of small amounts of $H_2PO_4^-$ to form $H_2P_2O_7^{2-}$. Potassium pyrophosphate formed in this manner and retained in the SCW effluent would also contribute to higher values of K/PO_4.

A question which must now be addressed is: How does the hydrolysis reaction affect the solubility of potassium phosphate? One method of examining this question is to evaluate the effect of hydrolysis on the solvation equilibrium constant, K_s, expressed in terms of activities (Dell'Orco, 1994). The solvation reactions for potassium hydroxide and potassium phosphate are given by eqs 4 and 5. The

$$KOH_{(L)} + nH_2O_{(SCF)} \rightleftharpoons KOH{\cdot}nH_2O_{(SCF)} \quad (4)$$

$$K_mH_{3-m}PO_{4(L)} + nH_2O_{(SCF)} \rightleftharpoons K_mH_{3-m}PO_4{\cdot}nH_2O_{(SCF)} \quad m = 1, 2, 3 \quad (5)$$

solutions considered here are dilute with respect to the solute, containing >99.9 mol % water. Because solute concentrations are generally so low, the activity of water is not expected to change. This leaves the activity of the solute and precipitated phase as the terms which might possibly change.

The activity of an associated electrolyte is essentially determined by its concentration and the ionic strength of solution. Previous studies (Mesmer et al., 1988) provide evidence that at water densities below 0.22 g·cm^{-3}, electrolytes can be considered as fully associated species, suggesting that the ionic strength is zero for these experiments. Unless the other solutes (KOH, H_3PO_4) or water have a strong physical interaction with potassium phos-

phate, it is unlikely that they affect its activity. The activity of the precipitated phase would be affected by a change in its composition. However, Figure 2 shows that the solubility of KOH was not exceeded during the phosphate studies. Any KOH formed during hydrolysis would be likely to remain in the SCF phase. The K/PO_4 ratio of the precipitated phase was between 1.8 and 1.9, suggesting that potassium in the precipitated phase was associated with HPO_4^{2-} and $H_2PO_4^-$. Thus, the effect of hydrolysis on the composition of the precipitated phase was limited to small changes in the relative amounts of mono- and dihydrogen potassium phosphate. The activities of the two phosphate species can be expected to be very similar, so that the effect of hydrolysis on the activity of the precipitated phase would also be small.

Another possibility which exists is that the hydrolysis reaction consumed enough potassium phosphate, by forming phosphoric acid, that the solubility limit of the SCF phase was not reached. This possibility is negated by the fact that rinse waters collected for all experiments showed an accumulation of potassium and phosphate, which indicated that precipitation occurred in all experiments. The pH of effluent samples was between 7 and 11, which also negates the possibility that significant amounts of phosphoric acid were produced from hydrolysis.

Electrolyte solubility is also influenced by the presence of high concentrations of corrosion products. Material corrosion was monitored by analyzing effluent and rinse water samples for iron, nickel, chromium, and molybdenum, the major elemental components of stainless steel. Iron and nickel were not recovered in any effluent or rinse water samples. Iron oxide (Fe_2O_3) and nickel oxide (NiO) are likely to be insoluble at both supercritical and ambient conditions, resulting in their collection by either of the effluent filters. In fact, reddish-brown particles were found on both effluent filters, indicating the presence of Fe_2O_3. The concentration of chromium and molybdenum was less than 2 ppm in all samples analyzed. Effluent samples were colorless. On the basis of the above observations, it was concluded that the presence of stainless steel corrosion products in the SCF phase did not have a significant effect on solubility measurements.

Toward the conclusion of the KOH experiments, representative samples of the effluent collected over the course of the study were analyzed by ICP for aluminum to evaluate the condition of the α-alumina ceramic packing. Aluminum concentrations varied between 100 and 300 ppm, indicating a gradual breakdown in the binding material of the alumina beads and a dissolution of the alumina crystals as $Al(OH)_4^-$. This was obviously not a desirable occurrence since high concentrations (>0.1 mol·L^{-1}) of other ionic species may enhance the solubility of an electrolyte in SCW by increasing the number of solute–solute interactions and thereby increasing the effect of the "nonaqueous" solvation mechanism (Valyashko, 1976). It is uncertain to what extent the dissolved aluminum hydroxide influenced the solubility of KOH. However, the highest observed concentration of aluminum was 0.01 mol·L^{-1}, which is 1 order of magnitude below the threshold concentration for solubility enhancement given above. Also, comparison of solubility data collected in a batch system with data from the packed bed apparatus suggests that the presence of dissolved aluminum did not significantly influence the solubility of KOH. The solubility of KOH measured in a 1 L autoclave reactor at 453 °C and 28.6 MPa in the absence of any packing material was 6.13×10^{-3} mol·kg^{-1}. This value was not significantly different from the value of 5.91×10^{-3} mol·kg^{-1} measured with the alumina bead chamber at 450 °C and 27.8 MPa. The difference in water density between the batch experiment (0.131 g·cm^{-3}) and the flow tests (0.129 g·cm^{-3}) could account for the difference in the two solubility measurements.

Table 4. Solvation Model Parameters from the Regression of Experimental Data in accordance with Eq 5

compound	n	K_s/(mol·L^{-1})^n	R^2
potassium hydroxide	3.03	1.37×10^{-5}	0.95
potassium phosphate	8.78	5.12×10^{-13}	0.95

For the potassium phosphate studies, the alumina packing was replaced with $^1/_{16}$ in. nickel wire cut into $^1/_4$ in. sections. Nickel and nickel alloys are resistant to corrosion in SCWO environments, in part due to the formation of a passivating nickel oxide layer (Matthews, 1991). Nickel corrosion products were not detected in the effluent samples or in the water used to rinse the apparatus between experiments. Visual inspection of the packing material following exposure to SCW and potassium phosphate showed no evidence of corrosion or erosion.

Analysis of Solubility Data

A common method for modeling electrolyte solubility in high-temperature water involves using a simple solvation mechanism to describe the equilibrium between the precipitated electrolyte and its component in the supercritical fluid phase (Martynova, 1976; Galobardes, 1981; Dell'Orco, 1994; Armellini and Tester, 1993). A complete derivation of the solvation model is provided in the above references, and therefore, only a brief description is given here.

The equilibrium constant for the solvation reaction, expressed in terms of activities, is simplified by defining the infinite dilution activity coefficients as unity, substituting density for the concentration of water, and assuming the activity of the precipitated electrolyte to be unity. The resulting expression for the equilibrium constant is

$$K_S \approx \frac{C_{X \cdot n H_2O}}{\varrho_{H_2O}^{\,n}} \tag{6}$$

where K_s = solvation equilibrium constant, (mol·L^{-1})$^{-n}$, $C_{x \cdot nH_2O}$ = concentration of solvated ion pair, mol·kg^{-1}, ϱ_{H_2O} = density of water, mol·L^{-1}, n = hydration number.

Taking the natural logarithm of both sides of eq 6 yields an expression suitable for regression of experimental data in the form of ln (solubility) versus ln (density)

$$\ln C_{x \cdot nH_2O} = n \ln \varrho_{H_2O} + \ln K_S \tag{7}$$

The slope (n) in eq 7 represents the number of water molecules required to solvate the associated electrolyte species in the supercritical fluid phase. The slope may or may not show a temperature dependence (Martynova, 1976). The y-intercept is proportional to the equilibrium constant (K_s), which is a function of temperature. Equation 7 predicts that isothermal plots of ln (solubility) versus ln (density) will yield a series of straight lines whose y-intercepts and slopes differ by some amount as a result of their temperature dependence. Additional data are necessary to accurately model the temperature dependence of K_s and n for potassium hydroxide and potassium phosphate.

Experimental solubility data for both compounds were regressed in accordance with eq 7, neglecting the temperature dependence of K_s and n. Table 4 shows the regression results. Correlation coefficients (R^2) for both regres-

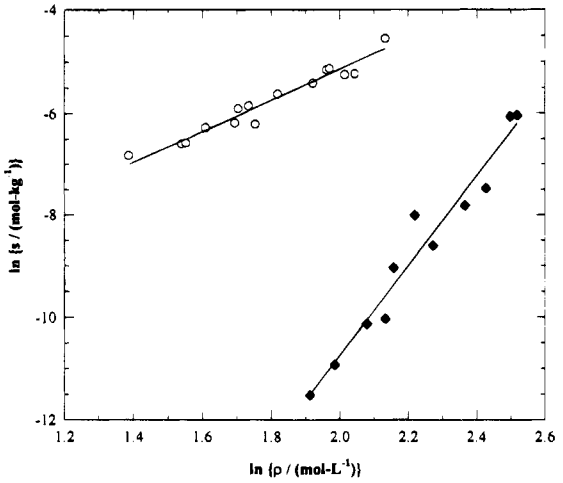

Figure 3. Comparison of experimental solubility values for potassium hydroxide (○) and potassium phosphate (◆) with those predicted by the solvation model (—).

sions were 0.95, indicating good agreement between experimental values and the solvation model. These results suggest that over modest temperature intervals only a small error is introduced by neglecting the temperature dependence of K_s and n. Figure 3 compares the measured solubilities of potassium hydroxide and potassium with values predicted from the solvation model.

The composition of the liquid melt can clearly affect the activity term in the expression for the equilibrium constant. This term was assumed to be unity in the derivation of eq 6, corresponding to a pure liquid salt phase. It is more likely that the liquid melt contained hydration water and small amounts of potassium precipitated corrosion products, resulting in an activity which deviated from unity. For example, Marshall (1981) reported that, in saturated liquid-solid solutions of potassium phosphate, the stable saturating solid contained between 0 and 0.5 mol of hydration water. The determination of the chemical composition of the liquid melt requires a more advanced method, such as a rocking autoclave. An activity coefficient which deviates from unity further limits the meaning of the parameter K_s in the semiempirical solvation model.

Conclusions

An experimental procedure for determining the solubility of low-melting electrolytes was successfully applied to the systems $KOH-H_2O$ and $K_2HPO_4-H_2O$. This procedure utilized a continuous-flow, packed-bed apparatus to achieve rapid precipitation and separation of electrolytes from the supercritical fluid phase. The results of the potassium phosphate study indicated that some potassium phosphate underwent hydrolysis. The significance of the hydrolysis reaction was addressed by evaluating the effect that hydrolysis products, KOH and H_3PO_4, had on the solvation equilibrium constant. The combination of very low electrolyte concentrations and the low ionic strength of supercritical salt–water solutions led to the conclusion that the effect of hydrolysis on the measured solubility of potassium phosphate was small. Finally, results were fit to a semiempirical solvation model to yield predictive equations for solubility as a function of water density. The simplified solvation mechanism adequately described the solubility behavior of potassium hydroxide and potassium phosphate over the temperature range of interest.

Literature Cited

Armellini, F.; Tester, J. Solubilities of Sodium Chloride and Sodium Sulfate in Sub- and Supercritical Water from 450–550 °C and 100–250 bar. *Fluid Phase Equilib.* **1993**, *84*, 123–142.

Connolly, J. Solubility of Hydrocarbons in Water Near the Critical Solution Temperature. *J. Chem. Eng. Data* **1966**, *11*, 13–16.

Dell'Orco, P. C. Reactions of Inorganic Nitrogen Species in Supercritical Water. Ph.D. Dissertation, University of Texas, Austin, TX, 1994.

Dell'Orco, P.; Gloyna E.; Buelow, S. The Separation of Solids From Supercritical Water Oxidation Processes. *Supercritical Fluid Engineering Science*; ACS Symposium Series 514; Washington D.C., 1993.

Galobardes, J.; Van Hare, D.; Rogers, L. Solubility of Sodium Chloride in Dry Steam. *J. Chem. Eng. Data* **1981**, *26*, 363–366.

Haar, L.; Gallagher, J.; Kell, G. *NBS/NRC Steam Tables*; Hemisphere Publishing Corp.: Washington, D.C., 1984.

Marshall, W. L. Conductances and Equilibria of Aqueous Electrolytes over Extreme Ranges of Temperature and Pressure. *Rev. Pure Appl. Chem.* **1968**, *18*, 167–186.

Marshall, W. L. Two-Liquid-Phase Boundaries and Critical Phenomena at 275–400 °C for High-Temperature Aqueous Potassium Phosphate and Sodium Phosphate Solutions. *J. Chem. Eng. Data* **1982**, *27*, 175–180.

Marshall, W.; Begun, G. Raman Spectroscopy of Aqueous Phosphate Solutions at Temperatures up to 450 °C. *J. Chem. Soc., Faraday Trans. 2* **1989**, *85* (12), 1963–1978.

Marshall, W.; Hall, C.; Mesmer, R. The System Dipotassium Hydrogen Phosphate-Water at High Temperatures (100–400 °C); Liquid-Liquid Imiscibility and Concentrated Solutions. *J. Inorg. Nucl. Chem.* **1981**, *43*, 449–455.

Martynova, O. I. Solubility of Inorganic Compounds in Subcritical and Supercritical Water. *High Temperature, High Pressure Electrochemistry*, 4th ed.; National Association of Corrosion Engineers: Houston, 1976, pp 131–138.

Mesmer, R. E.; et al. Thermodynamics of Aqueous Association and Ionization Reactions at High Temperatures and Pressures. *J. Solution Chem.* **1988**, *17* (8), 699.

Pitzer, K.; Pabalan, R. Thermodynamics of NaCl in Steam. *Geochim. Cosmochim. Acta* **1986**, *50*, 1445–1454.

Urusova, M. A. Phase Equilibria in the Sodium Hydroxide-Water and Sodium Chloride-Water Systems at 350–550 °C. *Russ. J. Inorg. Chem.* **1974**, *19* (3), 450–454.

Valyashko, V. M. Phase Equilibria in Water-Salt Systems: Some Problems of Solubility at Elevated Temperature and Pressure. *High Temperature, High Pressure Electrochemistry*, 4th ed.; National Association of Corrosion Engineers: Houston, 1976; pp 153–157.

Received for review November 3, 1994. Revised February 7, 1995. Accepted March 21, 1995.[⊗] Funding was provided by the Advanced Research Projects Agency (ARPA) and the U.S. Air Force.

JE940234W

[⊗] Abstract published in *Advance ACS Abstracts*, June 1, 1995.